*34th EPS Conference on Plasma Phys. Warsaw, 2 - 6 July 2007 ECA Vol.**31F**, P-1.052 (2007)*

Impurity Influx in the All Tungsten ASDEX Upgrade

R. Dux, R. Pugno, T. Pütterich, V. Bobkov, A. Kallenbach, R. Neu,
and the ASDEX Upgrade Team
Max-Planck-Institut für Plasmaphysik, EURATOM Association, Garching, Germany

Introduction

In ASDEX Upgrade, the transition from carbon based plasma facing components towards a full tungsten machine has been completed during the last vent, where the divertor strike point areas and remaining main chamber parts have been equipped with W-coated graphite tiles. Spectroscopic tungsten influx measurements are performed to identify the main source areas and to study the mechanisms that lead to tungsten production. Physical sputtering of tungsten by D has a high energy threshold [1] and for thermal plasma ions at typical plasma temperatures at the walls, impurity sputtering is the dominant mechanism. The total yield is thus a function of the impurity composition and the charge state distribution. For the main light impurities B, C, N and O, the yield strongly decreases with decreasing plasma temperature for T<10 eV. Sheath rectified electric fields due to ion cyclotron resonance heating (ICRH), cause an acceleration of the impurity ions in the plasma sheath and increase the yield. Sputtering by fast D ions from NBI has been previously studied [2]. Locally, it can be an important contribution, however, the total source is not very large.

Experimental setup

The poloidal cross section of ASDEX Upgrade in Fig.1 shows all positions of the presented impurity influx measurements by red circles. These positions are imaged by various optical heads inside the torus onto the entrance of 400 μm thick silica fibres, which guide the light to four spectrometers, that have been devoted to the detection of the WI line radiation at 400.9 nm. The whole setup is calibrated with an integrating sphere standard. The measured photon fluxes are transformed into ion fluxes by applying the number of ionisations per emitted photon, i. e. the (S/XB) value. For tungsten, (S/XB)=20 is used [3]. All spectrometers detect the light with CCD cameras and can simultaneously measure on several lines-of-sight. Poloidal profiles along ICRH limiters are recorded on 12 lines-of-sight with a repetition period of 3.4 ms. At Z=0.08 m, the toroidal profile along the limiter width is measured with 5 lines-of-sight. The outer divertor strike point is monitored by 6 lines-of-sight with temporal resolution of 8 ms. Another line-of-sight near the strike point is used for fast spectra recording with repetition times down to 100 μs. The small horizontal tiles at the entrance to the outer divertor were observed on 6 lines-of-sight with 1.9 ms resolution. In the standard setup, only carbon influxes at the central column are monitored on 18 lines-of-sight. During 31 discharges, the limiter spectrometer was used to measure W-influxes from the central column using every second line-of-sight. For these measurements, the exposure time had to be increased to 40 ms to detect the much lower flux

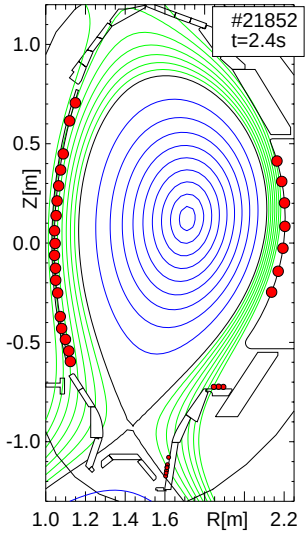

Fig.1: *Measurement locations for the presented tungsten fluxes.*

densities. Up to now, the inner divertor has not been observed, where tungsten erosion during ELMs is expected.

Tungsten erosion at the central column

The so called heat shield (HS) at the central column of ASDEX Upgrade is the largest plasma facing component with about 9.3 m^2. The heat shield has no protruding structures and the eroding ion flux is thus spread over a large area leading to rather low tungsten flux densities and accordingly low radiances of the tungsten line. Previously, tungsten influxes could only be detected, if the plasma was limited at the central column. During this campaign, the first measurements during diverted plasma operation succeeded.

In Fig.2, the tungsten influx distribution along the height of the heat shield is shown for an H-mode discharge with lower X-point and variation of the distance between separatrix and central column (I_p=800 kA, B_T=2.5 T for all discussed discharges). Throughout the paper, this distance is given by mapping the according location along the flux surface to the outer mid plane, i.e. to the height $Z = Z_{mag}$, where the difference $\Delta R = R - R_{sep}$ is determined. For all plasma facing components, decreasing distance to the separatrix leads to an increase of the sputtering flux density and to an increase of the yield due to the rising plasma temperature. This can be also seen on the distributions in Fig.2, where W shows a larger sensitivity to ΔR, i.e. shorter decay lengths, compared to B (boron is thought to be a remainder from previous campaigns, since there was no boronisation during this campaign). Below $Z \approx 0$ m, W influx densities are below the detection limit, which suggests, that the lower part of the central column is shielded by the upper part and that on the lower high field side, the power flux across the separatrix is not sufficient to cause high enough plasma temperatures in that region. During t =2.35-5 s, up to 2.1 MW of ICRH was added to the 7.5 MW of NBI heating, which leads to a noticeable increase of the tungsten erosion. The temporal resolution of 40 ms is too low, to judge whether sheath rectified electric fields cause this increase.

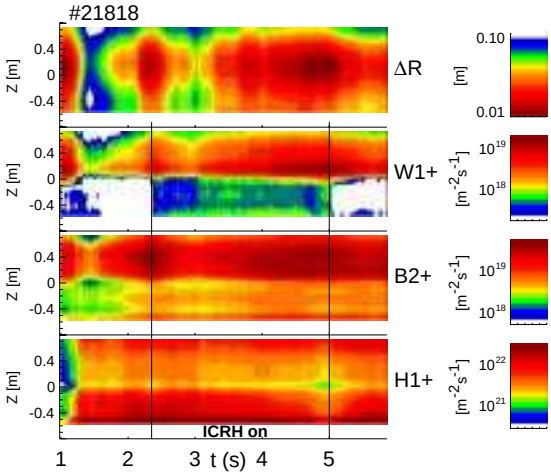

Fig.2: *Temporal evolution of the flux distribution along the heat shield for W, B, and H.*

Interpolation of the measured profile along the height of the central column allows to calculate the total tungsten source rate, which also shows a strong dependence on the minimum ΔR on the heat shield. For ΔR above 5 cm, which coincides with the distance, where the limiters are closer to the separatrix than the central column, the total source is below 10^{18} s^{-1}. For smaller distances the source rises to about 1.5×10^{19} s^{-1} at 2 cm for pure NBI heating and reaches up to 4×10^{19} s^{-1} with ICRH. The latter value is measured at the end of ICRH phase of the above discharge with ΔR=2.8 cm and 2.1 MW of ICRH.

Tungsten influx from the outboard limiters

From the twelve about 1 m high limiters at the outboard side, eight belong to the window frames around the four ICRH antennas, and four are at both sides of the two NBI ports. The quantification of the total tungsten source from these limiters by spectroscopic measurements is

approximative since not each limiter can be observed everywhere and since the erosion region on each limiter has a rather narrow toroidal extent in the range of 2 cm. Previously, it was not clear how far the W atoms travel from here before emitting the WI line, i.e. how much of the tungsten influx is seen by the spectroscopic measurement, which observes spots of 3.4 cm diameter. The toroidal width increases with the starting velocity, depends on the angular dependence of the velocity distribution, and decreases with rising electron density and temperature, where all quantities are not very well known. In the present setup, the toroidal extent of the emission cloud can be measured by 5 lines-of-sight positioned at the same height Z=0.08 m and separated toroidally by 1.9 cm at the limiter surface. The decay lengths, which are gained from these measurements, show the expected behaviour with lowest decay lengths for the lines from neutral species WI(400.9 nm), DI(410.0 nm) and HeI(402.6 nm) and higher values for the ion lines OII(407.5 nm) and BII(412.2 nm). An example is shown in Fig.3. The ratio of the toroidally integrated profiles and the calculated flux density for a spot size of 3.4 cm diameter is used for the integration of the total limiter source, assuming this ratio to be constant along the limiter height. The integration along the limiter height is done by linear interpolation between the different measurement locations, where values from different limiters at the same poloidal location are averaged.

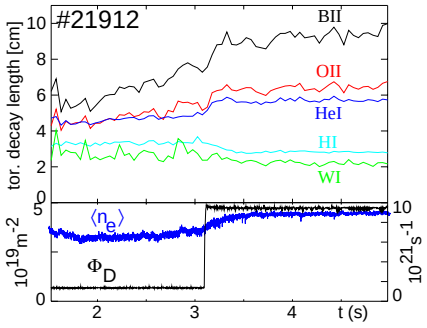

Fig.3: *Toroidal decay length of the line emission from neutral and singly ionised species at two density levels.*

Again, the distance to the separatrix is the most important parameter which determines the tungsten source at the limiter as can be seen in Fig.4. It depicts an almost repeat of discharge #21818 shown in Fig.2. Furthermore, a pronounced influence of ICRH is seen, which causes an abrupt change of the influx. The fluctuations are caused by ELMs, which, however, can not be resolved in this discharge with the 3.4 ms integration time of the camera. In this example, the heat shield source is always larger compared to the source rate from the 8 ICRH limiters. Fast particles from NBI do not contribute very much to the limiter erosion. Orbit calculations reveal, that the rather large distance to the separatrix causes the predominant fraction of the lost fast ions to be dumped into the divertor region (mainly on the roof baffle).

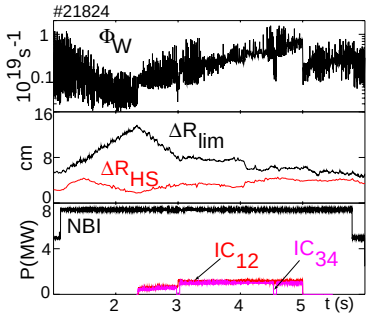

Fig.4: *Total tungsten source of the 8 ICRH limiter for a radial plasma sweep w/wo ICRH.*

Tungsten influx from the outer divertor

The outer divertor is the dominant tungsten erosion region. Here, the highest tungsten flux densities are observed during type-I ELMs, where the flux density can increase by a factor of 100 for cases with low divertor temperature before the ELM. The determination of the ELM averaged total source uses the 7 lines-of-sight on the strike-point plate close to the separatrix and 6 observations on the horizontal plate at the entrance to the divertor. The flux densities Γ_S, which are measured perpendicular to the poloidal divertor contour with co-ordinate S along the contour, are transformed to poloidal flux densities at the outer mid-plane $\Gamma_p =$

$\Gamma_S R(S) dS / R_{mid} dR_{mid}$, such that the influence of the flux expansion and the angle between the flux surface and the divertor contour is removed. Γ_p is quite well described by an exponential decay from the near SOL to the far SOL with decay lengths between 1 and 2 cm. Similar decay lengths have been found previously for the tungsten influx at the outboard limiters [4]. Using the fitted decay length, the profile along the complete outer divertor can be interpolated between these widely separated measurement positions. Profiles for two H-mode discharge with P_{NBI} =7.5 MW at low (#21852) and higher (#21818 as in Fig.2) level of deuterium puffing are shown in Fig.5. The separatrix distance of the start of the horizontal plate is indicated by a small vertical bar in Fig.5 (see also Fig.1). For the low puff case with ELM period of 13 ms, the total outer divertor source is 1.4×10^{20} s^{-1}, dropping to 6×10^{19} s^{-1} for #21818 with smaller, more frequent ELMs (3 ms). The later value is for the phase just after the ICRH. During the ICRH, the flux at the strike point module is unchanged, while at the horizontal plate the fluxes are approximately doubled. At the observed spots of the horizontal plates, the tungsten flux immediately (1.9 ms) reacts to the switching of the ICRH, however, independently of whether or not the magnetic field lines, that start at the spot, pass in the vicinity of the active antenna. Neglecting toroidal variations along the plate, a comparison of the different source regions yields for the influx change at t=5s in #21818 and #21824, that 2.1 MW of ICRH cause a change of about 5×10^{18} s^{-1} at the ICRH limiters, $\approx4\times10^{18}$ s^{-1} at the horizontal plate, and approximately 1.1×10^{19} s^{-1} at the inner heat shield.

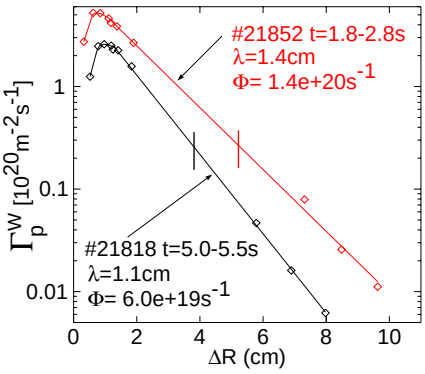

Fig.5: *Tungsten influx profiles in the outer divertor for low and high gas puff plotted versus the distance to the separatrix mapped to the outboard mid-plane.*

Finally, the contribution of the ELMs to the total flux densities was evaluated, which shall be described by the quantity $f_{ELM} = (\langle\Gamma\rangle - \Gamma_{off})/\langle\Gamma\rangle$ giving the part of temporally averaged flux $\langle\Gamma\rangle$, that is above the mean offset level Γ_{off} between ELMs. For #21852 with long ELM period of 13 ms, all outboard positions are measured with ELM resolution and yield: f_{ELM} =47% near the strike point, f_{ELM} =78% on the horizontal plate, and f_{ELM} =70% at the limiter. For #21818 with higher deuterium puff, the near SOL value is f_{ELM} =57%.

Carbon recycling at the central column

During the last vent, all tiles from the central column where mechanically cleaned to remove old deposition layers. Nevertheless, carbon recycling at the central column was detected right from the start of the campaign and since then, it has not decayed during the short duration of plasma operation. Due to the strong fluctuations caused by the varying plasma scenarios and geometries, long term changes of the carbon inventory are difficult to detect and would need a series of standard discharges, which have not yet regularly been performed.

References

[1] W. Eckstein, Tech. Report IPP 9/132, MPI für Plasmaphysik, Garching, Germany, 2002.
[2] R. Dux et al., J. Nucl. Mat., **363–365**, 112 (2007).
[3] A. Thoma, et al., Plasma Phys. Controlled Fusion **39**, 1487 (1997).
[4] R. Dux, et al, J. of Nucl. Mat. **337-339**, 852 (2005).